FEBS 27357

FEBS Letters 546 (2003) 195–202

Annexin AI processing is associated with caspase dependent apoptosis in BZR cells

R. Debret[a], H. El Btaouri[a], L. Duca[a], I. Rahman[b], S. Radke[c], B. Haye[a], J.M. Sallenave[d], F. Antonicelli[a,*]

[a] *Laboratoire de Biochimie, CNRS FRE 2534, Université de Reims Champagne-Ardenne, UFR Sciences, Moulin de la Housse, P.O. Box 1039, 51687 Reims Cedex 2, France*

[b] *COLT, Medical School, The University of Edinburgh, Edinburgh, UK*

[c] *ICGM, INSERM U 332, Paris, France*

[d] *Rayne Laboratories, Medical School, The University of Edinburgh, Edinburgh, UK*

Received 6 February 2003; revised 21 March 2003; accepted 28 March 2003

First published online 27 May 2003

Edited by Richard Marais

Abstract **Annexins are widely distributed and have been described in lung as well as in other cells and tissues. Annexin I (ANX AI) is a member of the calcium-dependent phospholipid binding protein family. Besides its anti-inflammatory function, ANX AI has been involved in several mechanisms such as the Erk repression pathway or apoptosis. To investigate the role of ANX AI on apoptosis in broncho-alveolar cells, we have constructed a plasmid containing the ANX AI full length cDNA. Transfected BZR cells displayed a higher level of both forms of ANX AI (37 and 33 kDa) as well as a decrease in cell viability (two-fold versus cells transfected with an empty vector). In order to analyse the endogenous ANX AI processing during stimulus-induced apoptosis, BZR cells were treated with a commonly used inducer, i.e. C2 ceramides. In these conditions, microscopic analysis revealed chromatin condensation in dying cells and the Bcl-2, Bcl-x_L/Bax mRNA balance was altered. Caspase-3 is one of the key executioners of apoptosis, being responsible for the cleavage of many proteins such as the nuclear enzyme poly-(ADP-ribose) polymerase (PARP). We demonstrate that caspase-3 was activated after 4 h treatment in the presence of ceramide leading to the cleavage of PARP. Dose–response experiments revealed that cell morphology and viability modifications following ceramide treatment were accompanied by an increase in endogenous ANX AI processing. Interestingly, in both ceramide and transfection experiments, the ANX AI cleaved form was enhanced whereas pre-treatment with the caspase inhibitor Z-VAD-fmk abolished ANX AI cleavage. In conclusion, this study demonstrates a complex regulatory role of caspase-dependent apoptosis where ANX AI is processed at the N-terminal region which could give susceptibility to apoptosis upon ceramide treatment.**

Key words: Annexin AI; Ceramide; Apoptosis; Caspase; BZR cell

1. Introduction

Structurally annexin AI (ANX AI) belongs to a family of ubiquitous phospholipid and calcium binding proteins. These proteins were initially described as potent inhibitors of phospholipase A2 (PLA2) activity whose synthesis is controlled by glucocorticoid synthetic hormones [1,2]. Later, ANX AI was implicated in several processes, of which some of the more attractive proposals include their involvement in the regulation of membrane trafficking and exocytosis [3,4], the mediation of cytoskeleton–membrane interactions [5,6], mitogenic signal transduction, cell proliferation and differentiation [7–12] as well as apoptosis [13,14]. However, despite detailed structural information, the biological functions of annexins are not clearly defined in vivo.

Apoptosis is an essential, highly conserved, and tightly regulated cellular process of cell death that is important for development, host defence and suppression of malignant transformation and inflammatory processes. Keeping apoptosis under control limits the survival of deranged cells, reducing the inflammatory processes. Membrane lipids of the sphingolipid class have long been assumed to be a mechanical barrier to the extracellular environment. However, it has been shown that ceramides, a second messenger [15], can be activated by receptor-mediated mechanisms [16], and play an essential role in cell growth, survival and death [17,18]. Indeed, ceramide has been shown to induce apoptosis in a number of different systems. Ceramide mediates apoptosis induced by environmental stresses, chemotherapeutic agents or by the tumor necrosis factor α receptor superfamily. Ceramide mimics the Fas pathway through Ras and mitogen-activated protein kinase (MAPK) phosphorylation, caspase activation and cell death.

The bronchial epithelium represents the last anatomic barrier between host and aggressive agents responsible for inflammatory and immunological reactions. Chronic inflammation diseases, such as cystic fibrosis, implicate ANX AI recruitment to antagonise the pyrogenic activity of cytokines [19,20]. In these conditions, a 33 kDa truncated form of ANX AI has been found in broncho-alveolar lavage fluid from patients next to protease activation [21]. Large amounts of ANX AI have also been observed in pulmonary metastasis [22]. Because of its high degree of vascularisation, the bronchial epithelium is an easy target for such secondary tumours. With regard to the importance of ANX AI in lung diseases, we have investigated the regulation of this protein in a broncho-alveolar cell line, BZR cells, and its relationship with the apoptotic phenotype. Thus, we have demonstrated that caspase activation is associated with a limited proteolysis of ANX AI in BZR cells.

*Corresponding author. Fax: (33)-3-26 05 31 68.
E-mail address: frank.antonicelli@univ-reims.fr (F. Antonicelli).

0014-5793/03/$22.00
doi:10.1016/S0014-5793(03)00570-2

2. Materials and methods

The biochemical reagents used in this study were purchased from Sigma, France, except where stated otherwise.

2.1. Cell culture conditions

The broncho-alveolar epithelial cell line BZR (ATCC CRL-9483) was kindly provided by Dr J.M. Polette (INSERM U 514, Reims, France). Adherent cells were maintained in continuous culture at 37°C, 5% CO_2 in Dulbecco's modified Eagle's medium (DMEM) (Gibco BRL, Life Technology) supplemented with 10% (v/v) heat-inactivated foetal bovine serum (FBS) (Dutscher, France), 100 U/ml penicillin, 100 μg/ml streptomycin.

For the assays, confluent monolayers of BZR cells were washed twice with phosphate-buffered saline (PBS), and trypsin EDTA solution was added to detach the cells. DMEM containing 10% FBS to neutralise the trypsin was added to the detached cells, which were centrifuged at $400\times g$ for 5 min. The cells were then resuspended in DMEM plus 10% FBS. BZR cells were seeded into six-well plates at 0.2×10^6 cells per well and incubated overnight at 37°C, 5% CO_2. The wells were rinsed twice with DMEM without FBS prior to treatment.

2.2. Experimental procedures

C2 ceramide, or C2 dehydroceramide (control) solutions (cat. no. 110145 and 219537, Calbiochem, France) were added to culture medium at a concentration from 5 μM to 60 μM in fresh medium, and incubated at 37°C for varying times.

Caspase inhibitor (Z-VAD-fmk, cat. no. G7231/2, Promega, France) was added 1 h before the addition of C2 ceramide, and maintained in the medium until the cells were harvested.

2.3. Ceramide extraction and analysis

Lipids were extracted in chloroform/methanol (2:1, v/v) and purified by column and thin layer chromatography according to Leray et al. [23]. Briefly, the lipid extract was fractionated on a 300 mg silicic acid column. The neutral lipids were eluted with 10 ml of chloroform, glycolipids, which contain ceramides, with 15 ml of acetone/methanol (9:1, v/v), and phospholipids with 10 ml of methanol. Ceramides were analysed on borate-impregnated LK5 plates (Whatman, Clifton, NJ, USA) with chloroform/ethanol/water/triethylamine (30/35/7/35, v/v) as the eluent and subsequently sprayed with 20% (v/v) H_2SO_4 solution in water. Ceramides were then visualised by charring during 15 min at 180°C.

2.4. Determination of cytotoxicity

The cytotoxic effect was evaluated directly on six-well culture plates using the tetrazolium-based 3-[4,5-dimethylthiazol-2-yl]-2,5-diphenyl-tetrazolium bromide (MTT) assay [24].

2.5. Determination of apoptosis

The degree of chromatin condensation was determined by fluorescent staining of living and dead cells by the use of the dye Hoechst 33258 on cells cultivated on six-well plates following the protocol given by the manufacturer (Molecular Probes).

For FACS analysis, cells were seeded in 75-cm^2 flasks and treated with C2 ceramide at a dose of 40 μM. After a period spanning 6–12 h, cells were washed twice with cold PBS and resuspended in buffer at a concentration of 5×10^6/ml: 5×10^5 cells were mixed with 2 μl of fluorescein isothiocyanate (FITC)-conjugated ANX V antibody (Roche Diagnostics, Mannheim, Germany) and 2 μl of 1 mg/ml propidium iodide (PI). After 15 min incubation at room temperature in the dark, and further washes, cells were diluted at a concentration of 10^5/ml. Samples were analysed by flow cytometry with a FACS analyser (FACSCalibur, Becton Dickinson) and a computer station running CellQuest software. ANX V staining was detected in the FL1 (green) channel, whereas PI staining was monitored in the FL2 (red) channel: appropriate quadrants were set and the percentages of cells negative for both stains (viable cells), positive for ANX V (apoptotic cells) and positive for PI (dead cells) were acquired.

Apoptosis was confirmed with mRNA and protein analyses.

2.6. Isolation of total RNA and mRNA expression studies (RT-PCR)

Total RNA was isolated from BZR cells using the TRIzol reagent (Invitrogen Life Technologies, Cergy Pontoise, France) following the manufacturer's recommendations and analysed on agarose gels stained with ethidium bromide.

Oligonucleotide primers were chosen using the published sequences of the human ANX AI [25], Bcl-2, Bcl_X, Bax [26] and 18S RNA [27]. Invitrogen Life Technologies synthesised the primers. The sequences of the primers, the annealing temperatures and the number of cycles used for the polymerase chain reaction (PCR) are summarised in Table 1. One microlitre of the reverse transcribed mRNA mixture was added directly to the PCR mixture and used for the PCR reactions containing 1 unit of Taq DNA polymerase (Promega, UK). The resulting PCR-amplified DNA fragments were confirmed by DNA sequencing. Bands were visualised and scanned using a white/UV gel camera Imaging densitometer, UVP (Bio-Rad, France).

2.7. Construction of the PDK-6-ANX AI vector and transient transfection of BZR cells

A cDNA encoding ANX AI was amplified using the PCR conditions described previously. The cDNA was endowed with a *Bam*HI restriction site on both its 5′ and its 3′ extremities (see primer sequence Table 1). The PCR product was ligated in-frame into the *Bam*HI restriction site of the PDK-6 vector [28]. Sense of insertion was defined using the *Eco*RV restriction site present at the 3′ extremity (1002 bp) and in the polylinker. The sequence of the PDK-6-ANX AI construct was verified by DNA sequencing.

Transfection of the PDK-6-ANX AI vector was carried out following the LipofectAMINE procedure as described by the manufacturer (Invitrogen Life Technologies). Transfected cells were maintained in DMEM supplemented with 10% FBS. Briefly, BZR cells (0.2×10^6 cells per well) were seeded into six-well tissue culture plates and cultured at 37°C to 40% confluence. Transfection was performed with 1 μg of PDK-6-ANX AI plasmid per well or with the empty PDK-6 vector for control. Following incubation, cells were stained or extracts were prepared and assayed for RNA or protein content.

2.8. Preparation of protein extracts

The medium overlying the cells was discarded and replaced with ice-cold PBS. BZR cells were harvested by scraping, followed by centrifugation at $400\times g$. Cells were lysed in PBS pH 7.4, 0.5% Triton X-100, 80 mM β-glycerophosphate, 50 mM EGTA, 15 mM $MgCl_2$, 1 mM Na_3VO_4 and protease inhibitors. Lysates were centrifuged for 20 min at $15\,000\times g$, and supernatants diluted in reducing sodium dodecyl sulfate (SDS) sample buffer. Protein content was determined using the BCA protein quantification kit (Interchim, France).

2.9. Western blotting of ANX I, caspase-3, poly(ADP-ribose) polymerase (PARP), Bax and Bcl-x_L

Proteins were separated on 10% acrylamide denaturing gels and transferred to nitrocellulose membranes. Blots were blocked with 10 mM Tris–HCl buffer (pH 7.5)/150 mM NaCl (Tris-buffered saline, TBS) with 5% non-fat dried milk for 45 min, and probed with either specific anti-ANX I (dilution 1:500), anti-caspase-3 (dilution 1:1000), anti-PARP (dilution 1:1000), anti-Bax (dilution 1:2000) or anti-Bcl-x_L (dilution 1:2000) antibodies in TBS containing 0.1% Tween 20 and 5% non-fat dried milk. After three washes with TBS 0.1% Tween 20, the membranes were incubated with an anti-rabbit secondary antibody, diluted at 1:4000 in TBS containing 0.1% Tween 20 and 5% non-fat dried milk. Three washes in TBS 0.1% Tween 20, and two washes in TBS were performed before visualisation. The ANX AI polyclonal antibody was a generous gift from Dr Russo-Marie. Caspase-3 (ref. no. 9662) and PARP (ref. no. 9542) antibodies were purchased from Cell Signalling Technology, Ozyme, France, Bax (cat. no. MS-711-P0) and Bcl-x_L (cat. no. MS-1346-P0) antibodies from Neomarkers.

3. Results

3.1. Effect of ANX AI on cell density

To provide evidence that ANX I is involved in the regulation of BZR cell viability, we transfected these cells with a full-length ANX AI cDNA plasmid construct (Fig. 1A). ANX AI over-expression was assessed at both the mRNA and protein levels. Compared to cells transfected with a negative control plasmid or with an ANX AI antisense plasmid, ANX AI-

Table 1

Gene	Sequence	Annealing temperature (°C)	Cycles	Expected Size
18S RNA	(S) 5′-gcgaattcctgccagtagcatatgcttg-3′ (AS) 5′-ggaagcttagaggagcgagcgaccaaagg-3′	55	26	126
Bcl-2	(S) 5′-ttctttgagttcggtggggtc-3′ (AS) 5′-tgcatatttgtttggggcagg-3′	55	30	304
Bcl_x	(S) 5′-ttggacaatggactggttga-3′ (AS) 5′-gtagagtggatggtcagtg-3′	55	30	600: Bcl_{xS} 800: Bcl-x_L
Bax	(S) 5′-gacccggtgcctcagga-3′ (AS) 5′-ccggaggaagtccaatgt-3′	55	30	294
ANX AI	(S) 5′-cgcggatcctcaaaaatggcaatggtatcag-3′ (AS) 5′-cgcggatccgcgacgcgttttattttcagctacatagac-3′	58	30	1344

transfected cells displayed a higher mRNA level measured at 24 h and protein level after 48 h (Fig. 1B,C). In these conditions, the limited-proteolysis form of ANX I was also enhanced in transfected BZR cells with the full-length ANX AI cDNA (Fig. 1C), while cell number decreased (Fig. 1C).

3.2. *Ceramide effects on cell morphology, cell viability and ANX AI expression*

Incubation of human broncho-alveolar cells (BZR cells) with C2 ceramide markedly affected their phenotype compared to the inactive dehydroceramide (Fig. 2A). The morphological changes in cells were dose-dependent leading to disruption of cell monolayer and were associated with rounded cells. Cells viability was also affected dose-dependently, with a percentage of survival cells relatively low after treatment with ceramide 40 μM for 24 h (Fig. 2B). In the same conditions, the expression of the ANX AI protein was examined using Western blotting with specific antibody. Following C2 ceramide treatment, the full-length ANX AI protein (37 kDa) level was barely affected, whereas the concen-

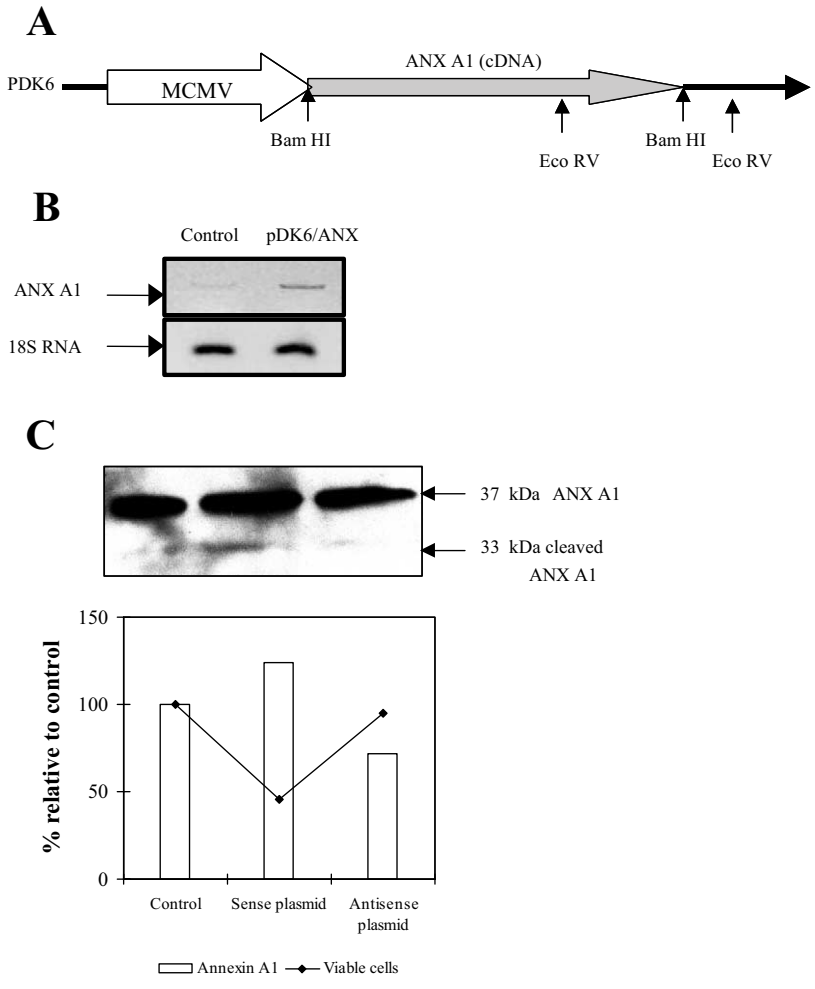

Fig. 1. ANX AI over-expression in BZR cells. Diagram of the PDK-6-ANX I vector. ANX AI cDNA expression is under the control of the SV40 promoter. *Bam*HI and *Eco*RV sites are delineated by arrows (A). ANX AI over-expression was assessed at the mRNA (B) and protein (C) levels after 24 and 48 h post-transfection respectively. The percentage of viable cells was determined by the MTT assay relative to control and percentage of ANX AI expression was determined by densitometric analysis (C). All experiments were performed in triplicate.

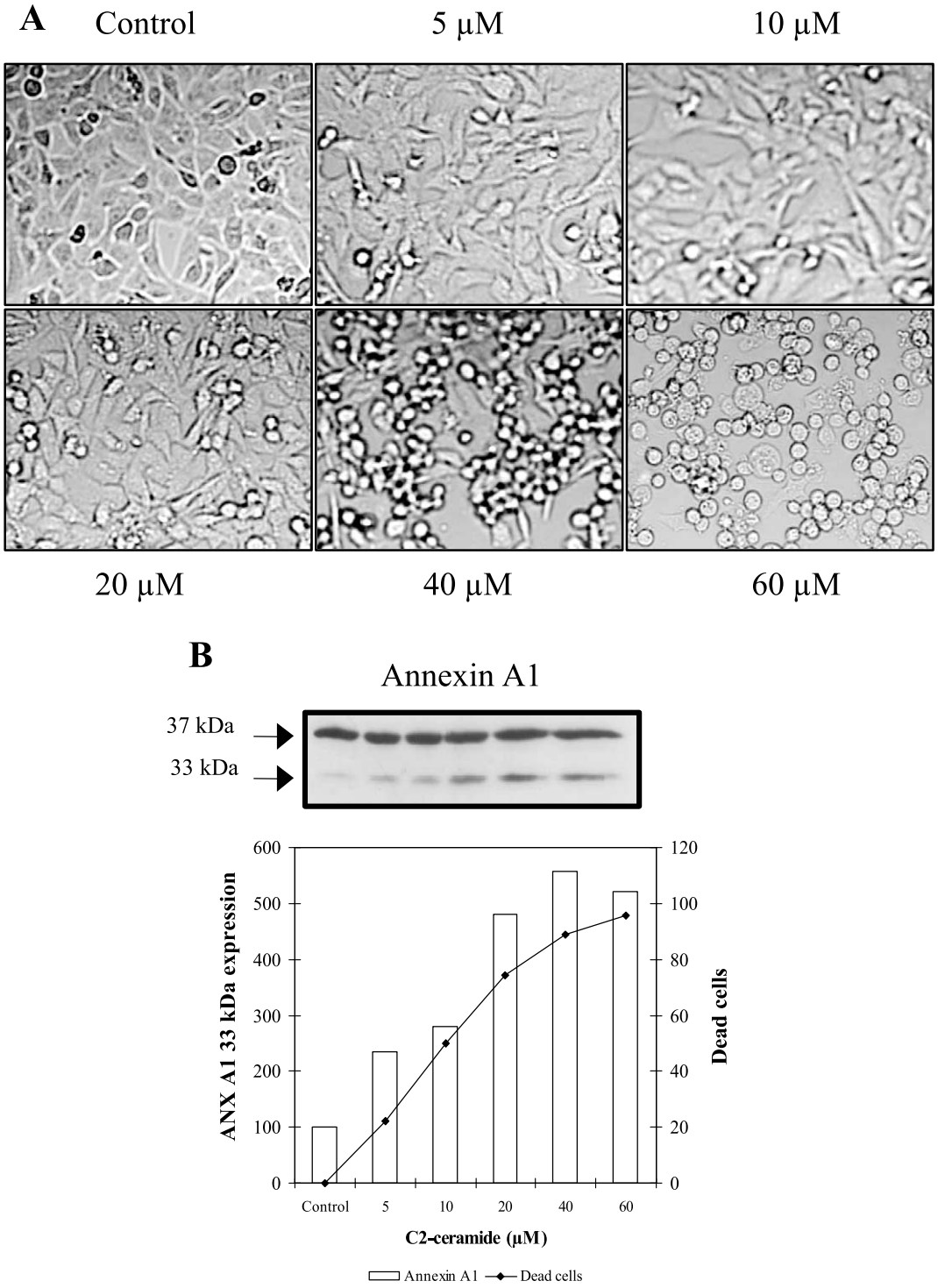

Fig. 2. Dose response of C2 ceramide on cell viability and morphology. BZR cells were treated with various concentrations of C2 ceramide for 24 h. A: Light microscopy (40×). B: Immunoblots were performed to detect ANX AI in BZR cells treated with dehydroceramide or with various concentrations of C2 ceramide. The amount in each protein samples was 40 μg. The percentage of viable cells was determined using the MTT assay. The deduced percentage of dead cells is shown on the left scale. Experiments were performed in triplicate.

tration of the N-terminally truncated protein (33 kDa) was dose-dependently increased (Fig. 2B). The degree of the ANX AI cleaved form paralleled cell death.

3.3. Ceramide effects on cell death

Kinetic study with a C2 ceramide concentration of 40 μM revealed that cell transformation was quite an early event (Fig. 3A,B). These cell modifications were associated with an increase in cytosolic C2 ceramide content (Fig. 3C). To investigate whether C2 ceramide-induced cell death corresponds to an apoptotic mechanism, apoptosis was further characterised by mRNA study of specific genes. Compared to control cells treated with dehydroceramide, Bcl-2 mRNA was weakly expressed in C2 ceramide-treated cells whereas

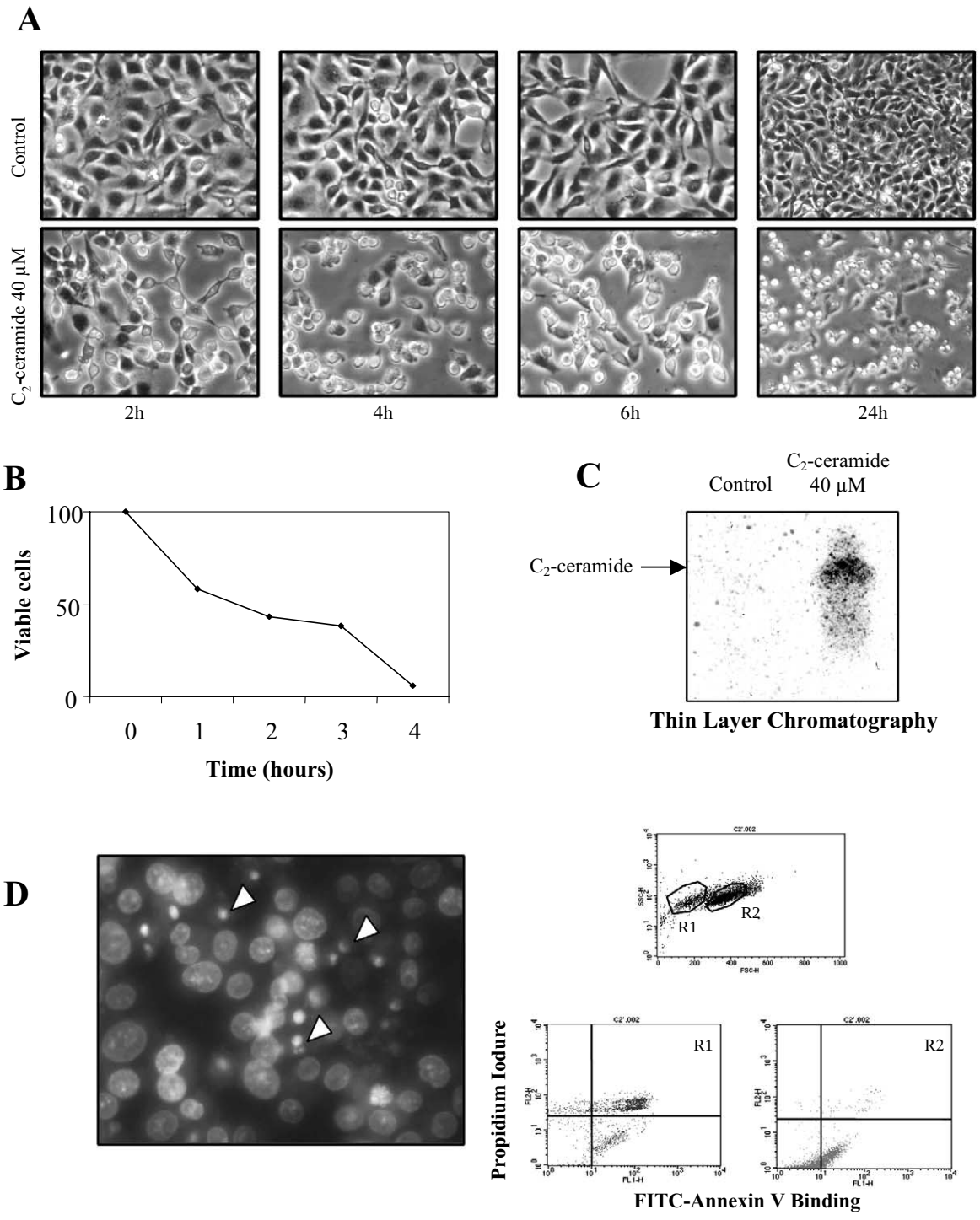

Fig. 3. Kinetics of action of C2 ceramide on BZR cells. BZR cells were treated with C2 ceramide (40 μM) for various times (from 0 to 24 h). A: Light microscopy (40×). B: The percentage of viable cells was determined using the MTT assay. C: C2 ceramide accumulation in the cytosol by thin layer chromatography. D: Chromatin condensation was defined after 16 h treatment with C2 ceramide (40 μM). Nuclear morphology was examined microscopically (40×) using the Hoechst dye. C2 ceramide-induced apoptosis was assessed by flow cytometry, and analysed for their staining in the FL1 channel (apoptotic cells labelled with ANX V-FITC) and/or in the FL2 channel (dead cells, positive for PI staining). Experiments were performed in triplicate.

Bax expression was enhanced (Fig. 4A). Due to differential splicing, the Bcl-x gene encodes two different proteins, a long Bcl-x_L and a short Bcl-x_S form which display opposite effects on cell survival (anti-apoptotic and pro-apoptotic respectively). In BZR cells, treatment with C2 ceramide (40 μM) led to an increase in the pro-apoptotic form while the anti-apoptotic form was not detected (Fig. 4A). Those gene modifications have been confirmed at the protein level using Bax and Bcl-x_L monoclonal antibodies (Fig. 4A). Cell staining with the DNA counter stain Hoechst dye shows that C2 ceramide (40 μM) caused condensation of chromatin in the nucleus while typical apoptotic phospholipid leaflet of cell mem-

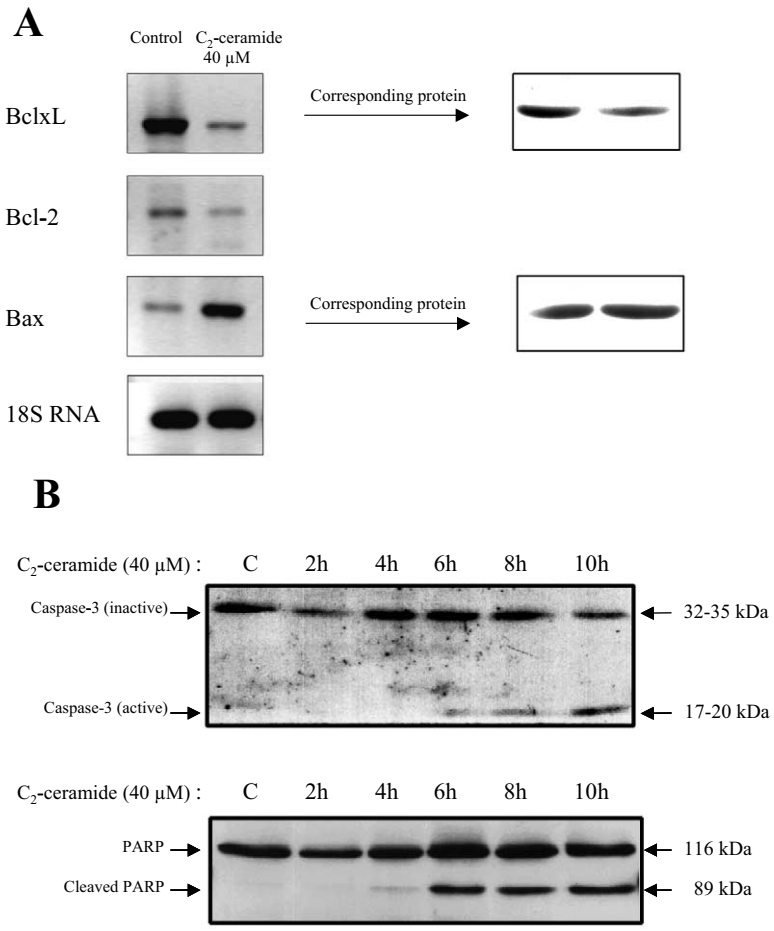

Fig. 4. C2 ceramide-induced apoptosis in BZR cells. A: BZR cells were treated with C2 ceramide (40 μM) or dehydroceramide (control) for 4 h. Expressions of pro-apoptotic (Bax) and anti-apoptotic (Bcl-2, Bcl-x_L) mRNAs were defined by reverse transcription PCR using the 18S RNA as housekeeping gene. Corresponding Bax and Bcl-x_L protein levels were obtained by Western blot (B). BZR cells were treated with C2 ceramide (40 μM) for various times. Cells were lysed and equal amounts of protein (40 μg) were loaded on a 10% SDS–polyacrylamide gel and immunoblotted with anti-caspase-3 or PARP antibodies.

brane was evidenced using ANX V-PI double staining (Fig. 3D). Finally, C2 ceramide-treated cells showed increased caspase-3 activation (Fig. 4B), with a marked protease activity observed by the cleavage of the nuclear enzyme PARP from 6 h after C2 ceramide (40 μM) had been added (Fig. 4B).

3.4. Effect of caspase activation on ANX AI-limited proteolysis

To further assess the relationship between ANX AI cleavage and caspase activation, BZR cells were pre-treated with the caspase-related apoptotic inhibitor Z-VAD-fmk. Addition of Z-VAD-fmk prior to transfection or C2 ceramide treatment blocked cleavage of ANX AI and impaired apoptotic morphological changes (Fig. 5A).

4. Discussion

Apoptosis is a mechanical programmed cell death triggered by a large variety of stimuli. However, common biological and morphological alterations are observed independently of the initial stimulus. This suggests that most of the signalling cascade events eventually converge on a restricted number of critical molecules. Hence, regulation of such switchboard molecules is of great interest in a strategy of cancer therapy. In this study, we report for the first time evidence that cleavage of the ubiquitous protein ANX AI is a target of the caspase activation cascade.

Transient transfection of human broncho-alveolar cells with a plasmid expressing the full-length ANX AI was associated with a decrease in viable cells. ANX AI has been proposed as a pro-apoptotic molecule and over-expression of full-length ANX AI has already been associated with cell death of the pre-monomyelocytic U937 cell line [13,14]. Nevertheless, we showed that in BZR cells ANX AI over-expression was associated with a processing of limited proteolysis. To investigate whether over-expression of ANX AI and/or its limited proteolysis were relevant for broncho-alveolar cell death we used a common apoptosis inducer, i.e. C2 ceramide, to study the relationship between apoptosis and ANX AI processing. An in vitro increase in intracellular ceramide concentration is generally associated with apoptosis induction [16,17]. In BZR cells, a high concentration of ceramide was required to induce apoptosis. However, this concentration is dependent on cell type. In 16-HBE cells, which are not h-Ras transfected and therefore present a weaker invasive potential [29], a concentration of ceramides of 20 μM was sufficient to induce cell death (data not shown). In vitro, an increase in cellular ceramide concentration is associated with apoptosis induction. Other metabolites may also contribute to the diverse action

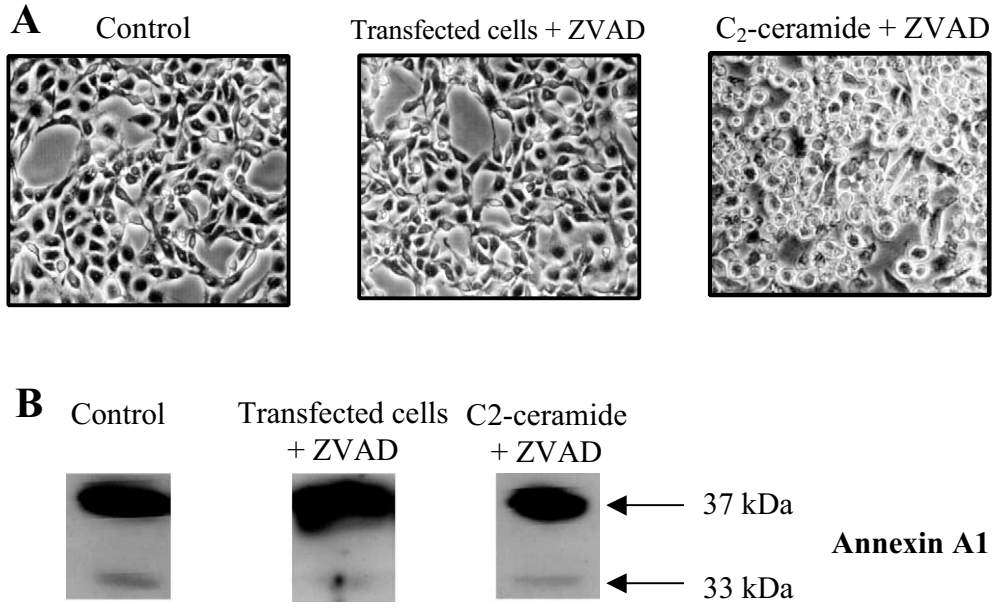

Fig. 5. C2 ceramide-induced apoptosis promotes ANX AI cleavage. BZR cells were pre-treated or not for 1 h with the caspase family inhibitor Z-VAD-fmk before addition of C2 ceramide 40 μM or transfection with the PDK-6-ANX I vector. A: Light microscopic examination of cells. B: Western blot analysis of ANX AI. The amount of protein loaded in each sample was 40 μg. Experiments were performed in triplicate.

of the sphingolipid class. While ceramide is often considered as anti-proliferative and pro-apoptotic, its metabolite, sphingosine-1-phosphate, has been implicated as a second messenger in cell growth [30], showing that the balance between these two sphingolipids is critical for determining cell survival or death. Determination of ceramide content after 6 h treatment showed an increase in C2 ceramide in treated cells compared to untreated cells confirming that: (i) C2 ceramide is cell membrane-permeant and (ii) it is a non-metabolisable compound. This result is also in keeping with the fact that a high concentration of ceramide is needed to induce apoptosis (Fig. 2) and that this required concentration is dependent on cell type. This observation raises the critical point that ceramides might directly regulate their death-activated pathways. Co-incubation with cycloheximide primes the ceramide apoptotic effect, showing that local protein post-transcriptional regulation is required for ceramide-induced apoptosis. In this setting, a decrease in human broncho-alveolar cell number was associated with morphological changes: chromatin condensation and membrane phospholipid flip-flop, as well as with cellular changes: caspase-3 activation, PARP cleavage and adequate Bcl-2, Bcl-x_L and Bax variations. In our model system, we showed that ceramide-induced apoptosis led to the ANX AI-limited proteolysis without significant variation of the full-length protein (37 kDa). Our work strongly supports the implication of ANX AI in ceramide-stimulated BZR cells, and points out the proteolytic cleavage of this protein as an important mechanism.

Interestingly, along with an increased expression of ANX AI, we also observed that the level of the cleaved form (33 kDa) was higher in cells transfected with the full-length ANX AI compared to control and to cells transfected with an antisense cDNA. It has been shown that the N-terminus of ANX AI can be cleaved at several positions by different proteases such as cathepsin D, calpain, plasmin and neutrophil elastase [21,31]. To provide an explanation for such an effect in our model system, we proposed ANX AI as a target of a caspase-activated cascade. In support of this hypothesis, we demonstrated that the peptide caspase inhibitor Z-VAD-fmk inhibited both ceramide-induced apoptosis and ANX AI-limited proteolysis. Therefore, we showed for the first time that caspase cascade inhibition is associated with a decrease in ANX AI-limited proteolysis. While further experiments are needed to address ANX AI processing, it seems unlikely that ANX AI is cleaved by a direct action of either group I (caspases 1, 2, 4, 5, 11), group II (caspases 6, 8, 9, 10) or group III (caspases 2, 3, 7) caspases since their recognition motifs are not present on the ANX AI translated sequence [25].

Considering that different properties might be bound to ANX AI multi-forms, we then considered the effect of such a cleavage on cell physiology. Over-expression of full-length ANX AI has been associated with cell death and caspase-3 activation [14]. Knowing that cPLA2 is a substrate of caspase-3 [32], this indirect anti-PLA2 mechanism of ANX AI should lead to a decrease of the anti-apoptotic molecule prostaglandin E2 (PGE2) production and therefore reinforce the ANX AI pro-apoptotic potential. Furthermore, caspase-3 also promotes ANX AI-limited proteolysis, leading to the N-terminally deleted ANX AI which still exhibits anti-PLA2 activity [33] and to the N-terminus peptide release presenting the EQEYV sequence which can act as a decoy substrate at the receptor level, blocking the association of Grb2, p21 (Ras) and Raf [34,35] and subsequently downstream activation of enzymes such as cPLA2. This inhibitory effect is in keeping with other studies showing that ANX AI-derived N-terminus peptide dose-dependently inhibits cytochrome oxidase 2 expression and PGE2 production [36] as well as that the N-terminus ANX AI peptide increases susceptibility to apoptosis [14]. Consequently, the assumed indirect cleavage of ANX AI via caspase activation leads the cell into a perpetuated circle ending with cell death. ANX AI could play a major role in tumour growth through the combination of several properties acting in concert: (1) on cell proliferation, which could be linked to its MAPK inhibitory effect, (2) on inflammation,

through its anti-PLA2 activity whether via direct [1] or indirect [37] mechanisms as well as through the decoy action of the N-terminus peptide [34–36] and the degradation of PLA2 by caspase-3 [32], and (3) on apoptosis by activation of the caspase-3 protease [14].

Most cancer cells continually develop abnormalities. Thus, a potential therapy that targets one specific cell type or cancer state may not eventually be efficacious. By contrast, in this study we provided evidence that ANX I is one potential intermediate molecule involved in the activation of biochemical programmes of cell growth arrest. We thus speculate that in human broncho-alveolar cells, the ceramide-induced cascade leading to cell death may be magnified through the ubiquitous intermediate ANX I involved in all mechanisms listed above.

Acknowledgements: CNRS, ARERS and the Comité de l'Aube de la Ligue contre Le Cancer supported this work. R.D. is the recipient of a bursary from the French government (Ministère de l'Education Nationale et de la Recherche). The authors are greatly indebted to Dr W. Hornebeck for critically reviewing the manuscript, and to Miss F. Wrisez for her kind technical participation.

References

[1] Hirata, F. (1981) J. Biol. Chem. 256, 7730–7733.
[2] Antonicelli, F. et al. (1988) FEBS Lett. 235, 252–256.
[3] Ali, S.M., Geisow, M.J. and Burgoyne, R.D. (1989) Nature 340, 313–315.
[4] Drust, D.S. and Creutz, C.E. (1988) Nature 331, 88–91.
[5] Zokas, L. and Glenney Jr., J.R. (1987) J. Cell Biol. 105, 2111–2121.
[6] Croxtall, J.D., Waheed, S., Choudhury, Q., Anand, R. and Flower, R.J. (1993) Int. J. Cancer 54, 153–158.
[7] Fava, R.A. and Cohen, S. (1984) J. Biol. Chem. 259, 2636–2645.
[8] Rainteau, D.P., Weinman, S.J., Kabaktchis, C.A., Smith, V.L., Kaetzel, M.A., Dedman, J.R. and Weinman, J.S. (1988) J. Biol. Chem. 263, 12844–12848.
[9] Schlaepfer, D.D. and Haigler, H.T. (1990) J. Cell Biol. 111, 229–238.
[10] Antonicelli, F., Omri, B., Breton, M.F., Rothhut, B., Russo-Marie, F., Pavlovic-Hournac, M. and Haye, B. (1989) FEBS Lett. 258, 346–350.
[11] Elbtaouri, H., Antonicelli, F., Claisse, D., Delemer, B. and Haye, B. (1994) Biochimie 76, 417–422.
[12] el Btaouri, H., Claisse, D., Bellon, G., Antonicelli, F. and Haye, B. (1996) Eur. J. Biochem. 242, 506–511.
[13] Canaider, S., Solito, E., de Coupade, C., Flower, R.J., Russo-Marie, F., Goulding, N.J. and Perretti, M. (2000) Life Sci. 66, PL265–PL270.
[14] Solito, E., de Coupade, C., Canaider, S., Goulding, N.J. and Perretti, M. (2001) Br. J. Pharmacol. 133, 217–228.
[15] Okazaki, T., Bielawska, A., Bell, R.M. and Hannun, Y.A. (1990) J. Biol. Chem. 265, 15823–15831.
[16] Okazaki, T., Bell, R.M. and Hannun, Y.A. (1989) J. Biol. Chem. 264, 19076–19080.
[17] Hannun, Y.A., Luberto, C. and Argraves, K.M. (2001) Biochemistry 40, 4893–4903.
[18] Kolesnick, R. (2002) J. Clin. Invest. 110, 3–8.
[19] Carey, F., Forder, R., Edge, M.D., Greene, A.R., Horan, M.A., Strijbos, P.J. and Rothwell, N.J. (1990) Am. J. Physiol. 259, R266–R269.
[20] Strijbos, P.J., Hardwick, A.J., Relton, J.K., Carey, F. and Rothwell, N.J. (1992) Am. J. Physiol. 263, E632–E636.
[21] Tsao, F.H., Meyer, K.C., Chen, X., Rosenthal, N.S. and Hu, J. (1998) Am. J. Respir. Cell Mol. Biol. 18, 120–128.
[22] Pencil, S.D. and Toth, M. (1998) Clin. Exp. Metast. 16, 113–121.
[23] Leray, C., Pelletier, X., Hemmendinger, S. and Cazenave, J.P. (1987) J. Chromatogr. 420, 411–416.
[24] Denizot, F. and Lang, R. (1986) J. Immunol. Methods 89, 271–277.
[25] Wallner, B.P. et al. (1986) Nature 320, 77–81.
[26] Bruggers, C.S., Fults, D., Perkins, S.L., Coffin, C.M. and Carroll, W.L. (1999) J. Pediatr. Hematol. Oncol. 21, 19–25.
[27] Sasaki, K., Hattori, T., Fujisawa, T., Takahashi, K., Inoue, H. and Takigawa, M. (1998) J. Biochem. (Tokyo) 123, 431–439.
[28] Sallenave, J.M., Xing, Z., Simpson, A.J., Graham, F.L. and Gauldie, J. (1998) Gene Ther. 5, 352–360.
[29] Polette, M., Gilles, C., de Bentzmann, S., Gruenert, D., Tournier, J.M. and Birembaut, P. (1998) Clin. Exp. Metast. 16, 105–112.
[30] Olivera, A. and Spiegel, S. (1993) Nature 365, 557–560.
[31] Ando, Y., Imamura, S., Hong, Y.M., Owada, M.K., Kakunaga, T. and Kannagi, R. (1989) J. Biol. Chem. 264, 6948–6955.
[32] Atsumi, G., Tajima, M., Hadano, A., Nakatani, Y., Murakami, M. and Kudo, I. (1998) J. Biol. Chem. 273, 13870–13877.
[33] Kim, S., Ko, J., Kim, J.H., Choi, E.C. and Na, D.S. (2001) FEBS Lett. 489, 243–248.
[34] Croxtall, J.D., Choudhury, Q. and Flower, R.J. (2000) Br. J. Pharmacol. 130, 289–298.
[35] Alldridge, L.C., Harris, H.J., Plevin, R., Hannon, R. and Bryant, C.E. (1999) J. Biol. Chem. 274, 37620–37628.
[36] Minghetti, L., Nicolini, A., Polazzi, E., Greco, A., Perretti, M., Parente, L. and Levi, G. (1999) Br. J. Pharmacol. 126, 1307–1314.
[37] Davidson, F.F., Dennis, E.A., Powell, M. and Glenney Jr., J.R. (1987) J. Biol. Chem. 262, 1698–1705.